Uncertainty and sensitivity analysis of modeling plant CO₂ exchange in the built environment

Peiyuan Li^a and Zhi-Hua Wang^a

^a School of Sustainable Engineering and the Built Environment, Arizona State University,

Tempe, USA

Corresponding author: Zhi-Hua Wang (zhwang@asu.edu)

† Tel: 1-480-727-2933; Fax: 1-480-965-0577

Abstract

1

2

3

4

5

6

7

8

9

10

11

12

13

14

The dynamics of carbon dioxide (CO₂) exchange in the built environment, coupled with local microclimate modeling, is of critical importance to the understanding of emergent patterns of longterm urban climate evolution. In addition to the complex model physics, the difficulty is outstanding to characterize uncertainties inherited in the parameter space and its impact on the model performance and predictive skills. In this study, we conducted a series of numerical simulations based on advanced Markov chain Monte Carlo algorithms to quantify the sensitivity of a recently developed modeling framework by coupling the dynamics of CO₂ transport into a single-layer urban canopy model. The results show that urban morphology (canyon aspect ratio), irrigation, and the physiological properties of urban vegetation predominate the processes of plant CO₂ exchange in the built environment. In contrast, the CO₂ budget is relatively insensitive to material properties of urban facets in the built environment. The findings in this study can help to unravel the interplay of urban carbon dynamics and the built environment, as well as to inform researchers and policy makers for sustainable urban development towards a low carbon city. **Keywords:** Carbon exchange; Markov chain Monte Carlo; Model sensitivity; Plant physiology;

- 17 Soil respiration; Urban environment

1 Introduction

Globally, urban areas cover approximately 3% of global land surface area but contribute ~70% of anthropogenic carbon dioxide (CO₂) emissions mainly through fossil fuel burning [1]. The carbon dynamics of urban areas entices complex interplay among anthropogenic and biospheric processes [2] via multiscale land-atmosphere interactions. Local urban microclimates modify the overlying urban boundary layer dynamics, such as the boundary layer height and thermal stratification [3, 4] which in turn impacts the spatio-temporal patterns of CO₂ variability over built terrains. For example, the transportation network of a city leads to enhanced CO₂ flux due to vehicular emissions, whereas on the other hand, the excessive heating over paved road surfaces contributes to raise the height of mixing layer and reduce the CO₂ concentration in the overlying atmosphere.

Among various sources and sinks of CO₂ exchange, urban vegetation, e.g. green roofs, street trees, urban lawns, golf courses, backyard gardens, etc., and their physiological functions emerge as the most challenging component for numerical modeling. Urban vegetation behaves distinctively from plants in the natural environment, primarily due to their peculiar growing conditions in the built environment. It is noteworthy that urban areas usually furnish favorable conditions for plant growth and physiological functions, because in cities: 1) warmer ambient temperatures, e.g. those due to the prominent urban heat island effect, allow urban plants to maintain a higher photosynthesis rate and a longer growing period [5-7]; 2) regular maintenance practices, such as irrigation and fertilization, relieve much of environmental stresses for plant growth [8]; and 3) the elevated CO₂ level forms a natural CO₂ pump, promoting the carbon assimilation rate [9, 10].

Among urban vegetation, urban trees have the most sophisticated biophysical functions, partially due to the complexity of their geometry (three dimensional as compared the planar distribution of grasses). Previous studies have found that the presence of street trees significantly alter the microclimate and the heat and moisture re-distribution in the urban canyon, including the change of surface energy balance [11], the reduction of thermal discomfort [12, 13], and weakening the passive pollutant dispersion [14], to name a few. In particular, urban trees influence CO₂ dynamics in counteracting ways: they are effective carbon sinks via photosynthesis, but meanwhile can also create unfavorable growing conditions for shaded ground vegetation (e.g. lawns). The shading effect tends to intercept solar radiation for photosynthesis and lower the ground level temperature [15-17], hence reduces the carbon uptake via ground vegetation by impeding their physiological functions.

The complex interplay between carbon dynamics and anthropogenic activities in urban areas can be partially captured in field measurements at sub-urban scale, e.g. flux towers deployed in different cities [18-20]. In addition, regional CO₂ exchange can be quantified via data fusion. For example, FluxCom uses machine learning algorithm to estimate global CO₂ flux by fusing in-situ eddy covariance measurements, satellite imagery, and global meteorological data [21]. This method is capable of producing reasonable carbon estimate in natural area or agriculture fields. When applied to urban areas, however, the characteristics of the built environment (e.g. urban morphology) are largely missing in the existing data fusion models, leading to large uncertainties in final data product. On the other hand, for urban CO₂ estimate, spatial gridded datasets are mostly focused on anthropogenic emissions exclusively, such as traffic emissions, power generation, cement production, etc. [22-24], leaving the biogenic carbon exchange unaccounted.

Given its dynamic complexity, up to date the quantification of urban carbon exchange largely resorts to observational dataset [18-20, 25], while physically based modeling remains at its infancy. Only until very recently, attempts have been made to incorporate CO₂ transport into single-layer urban canopy models (UCMs) [26, 27]. This family of UCMs provides a versatile and reasonably realistic modeling framework for parameterizing surface processes of heat, moisture, and scalar transport in the built environment [28-31]. By incorporating the CO₂ exchange in UCMs, the coupled modeling framework enables us to capture the interactions of dynamic transport of urban carbon emission and the local hydroclimate. In particular, the model developed by Goret et al. [26] has been focused on anthropogenic carbon release. In contrast, the model developed by Li and Wang [27] (hereafter referred to as the coupled UCM-CO₂ model) is more comprehensive with emphasize on plant physiological response to the urban environment. Both models have been extensively calibrated and evaluated against field observation of urban CO₂ emissions at specific cities. Nevertheless, uncertainties in the parameter space of the coupled UCM-CO₂ modeling framework remain unexplored and model sensitivity obscure.

It remains imperative for comprehensive sensitivity analysis to be conducted to better characterize the parameterization schemes in the coupled UCM-CO₂ model. But the conventional sensitivity analysis, viz. by quantifying changes in model output while tuning individual input parameters one at a time, presents numerical difficulties for this task. The major difficulties include: (1) the large number of parameters (hence the high dimensionality of the parameter space) in the coupled UCM-CO₂ model that can be broadly grouped as urban morphology, thermal properties of engineered materials, plant physiological properties, and soil hydrothermal properties, hence the conventional sensitivity analysis easily falls prey to the "curse of

dimensionality" [32], and (2) uncertainties in individual parameters inherent from variability of locations of cities and their local climatic and environmental conditions.

To break free from these difficulties, stochastic algorithms are usually resorted to in order to characterize parameter uncertainties and sensitivity of models involving complex system dynamics [33]; one particular method being the subset simulation using an advanced Markov chain Monte Carlo (MCMC) algorithm [34, 35]. Based on Bayesian inference, the MCMC algorithm improves the efficiency in the generation of conditional samples, which is particularly preferable for assessments of the tail of the probability distributions, viz. extreme events and risk analysis. It also produces less autocorrelation when dealing with multi-dimensional problems when comparing to the direct Monte Carlo (DMC) simulation. The subset simulation algorithm has been extensively applied for advanced sensitivity study of modeling frameworks adopting the single-layer UCM [4, 36, 37].

In this study, we characterize uncertainties in the parameter space in the newly developed coupled UCM-CO₂ model [27], and quantify the model sensitivity using the MCMC algorithm of subset simulation. The results of numerical simulations help to unravel the interactions among various determinants of urban carbon exchange processes, including urban morphology, soil status, landscape properties, and plant physiological functions. The current study also demonstrates the robustness of the new UCM-CO₂ model by estimating the plant dynamics under various urban settings. Results of the proposed sensitivity analysis with quantified uncertainties in the model parameter space will enable us to answer questions such as or how the urban morphology influence plant uptake of CO₂? Or what the co-benefit of mitigating heat and carbon emissions is by urban greening. The quantified model sensitivity will also be helpful as to

guide future development of modeling urban CO₂ exchange, or to inform urban planners and policy makers for a better decision towards a carbon neutral city.

2 Method

2.1 The UCM-CO₂ model

Single-layer UCMs are widely used in land surface modeling for cities all around the world (e.g. [38]) for its tractable parameter sensitivity [36, 39] and reliable performance [40, 41]. The historical development of UCMs was primarily focused on resolving urban land surface energy and moisture exchanges. It was only until very recently that attempts were made in incorporating plant physiological model and gridded CO₂ emission data in single-layer UCMs for capturing carbon exchange in urban area [26, 27]. Among all possible carbon sources/sinks in cities, the anthropogenic sources and their spatiotemporal pattern depend heavily on the population density and human activities rather. In contrast, the physiological functions of urban plant, especially trees, are primarily controlled by environmental conditions and their numerical modeling presents particular challenges.

More specifically, capturing the dynamics of urban vegetation in UCMs is complicated due to: (1) the numerical difficulty in representation of realistic tree geometry hence its participatory role in radiative exchange inside street canyons [42, 43], (2) the complexity of plant biophysical functions for transport of energy, moisture, and pollutants [14, 44], and (3) the lack of comprehensive parameterization schemes of urban CO₂ exchange by urban vegetation.

In this study, we adopt the newly developed UCM-CO₂ modeling framework [27] that incorporates plant physiological functions in urban land surface model and prognostically solves time-varying urban carbon fluxes arising from anthropogenic, biogenic, and soil sources/sinks

under local micrometeorological conditions. Moreover, the model differentiates urban trees from ground vegetation (e.g. lawns): individual plant type is subject to variable meteorological conditions, specific to its location in the street canyons, and modeled separately with corresponding biophysical functions of radiative heat exchange, evaporative cooling, and CO₂ dynamics. In particular, urban trees are defined by crown sizes and locations in street canyons, independent of those dimensional parameters of ground level vegetated area. The incorporation of urban trees in the UCM is therefore representative of more realistic setting of the built environment.

130

131

132

133

134

135

136

137

138

139

140

141

142

143

144

145

146

147

148

149

150

151

152

Here we briefly describe the coupled UCM-CO₂ model, with emphasis on the parameterization schemes that are most relevant to carbon exchange in urban areas. More detailed algorithms of the early development of this specific single-layer UCM for modeling urban land surface processes of energy, moisture, and scalar transport can be found in prior studies [17, 30, 37]. Figure 1 shows a schematic of the representative street canyon used in this study. The built terrain is represented as a generic unit of two-dimensional (2D) street canyon, consisting of two arrays of buildings separated by a road, with infinite longitudinal dimension. The in-canyon transport of energy, water, and scalar fluxes are resolved separately for each subfacet (walls, impervious and vegetated roads, shade trees, etc.). The street canyon includes two symmetric rows of trees with circular crown geometry for simplicity. The urban morphology is determined by the roof width (r), road width (w), and building height (h), normalized by the total (roof + road) width of the street canyon. The surface heterogeneity at the ground (road) level is represented using fractions of impervious pavement (f_p) , vegetation (f_v) , and bare soil (f_s) , each normalized by the road width (w), with $f_p + f_v + f_s = 1$ (Fig. 1). Tree parameters are normalized by canyon geometry: the tree crown radius r_T is normalized by road width w, the tree height h_T by

building height, and the relative distance between tree to the near wall x_T by half canyon width (with $x_T = 0$ the closest to the wall and $x_T = 1$ closest to the canyon center).

Driven by micrometeorological conditions, the UCM-CO₂ model calculates the gross primary production (GPP, total CO₂ assimilation via photosynthesis) using the *An-g*_c method [27, 45], given as

$$GPP = \left(A_m + R_d\right) \left(LAI - \frac{E_{int}}{K_x}\right), \tag{1}$$

where GPP is the CO₂ assimilation rate at canopy level; A_m is the plant primary productivity at leaf level; R_d is the plant dark respiration and usually calculated as a fraction of A_m ; LAI is the leaf area index; K_x is the extinction coefficient; and E_{int} represents the overall leaf density from top to bottom of the canopy, calculated as

163
$$E_{\text{int}} = \text{Ei}\left[\frac{\alpha K_x PAR}{A_m + R_d} \exp\left(-K_x LAI\right)\right] - \text{Ei}\left[\frac{\alpha K_x PAR}{A_m + R_d}\right], \tag{2}$$

with Ei [•] the exponential integral and *PAR* the photosynthetic active radiation, representing the
amount of radiation that is able to drive photosynthesis. The leaf level primary productivity (*A*_m)
is given by

$$A_{m} = A_{m,\text{max}} \left[1 - \exp\left(-g_{m} \frac{C_{i} - \Gamma}{A_{m,\text{max}}}\right) \right], \tag{3}$$

where $A_{m,\max}$ is the maximum primary productivity under high CO₂ concentration and sufficient light condition; g_m is the stomatal conductance; C_i is CO₂ concentration inside of leaves; and Γ is the CO₂ compensation point. Here $A_{m,\max}$ and g_m are temperature-dependent, and can be estimated using the Q_{10} -type method as

172
$$V_k(T_{leaf}, T_1, T_2) = V(T_{leaf}) \left\{ 1 + \exp\left[0.3(T_1 - T_{leaf})\right] \right\}^{-1} \left\{ 1 + \exp\left[0.3(T_{leaf} - T_2)\right] \right\}^{-1}, \tag{4}$$

where V_k is the temperature-dependent variable (in this case, $A_{m,\max}$ and g_m); $V(T_{leaf})$ is generic temperature-dependent variable; and T_1 and T_2 are empirical parameters for given types of plants [45].

Soil respiration is primarily regulated by soil temperature (T_s) and soil water content (θ), given as

178
$$R_{\text{soil}}(T_s, \theta) = f(\theta) R_{25} Q_{10}(T_s)^{(T_s - 25)/10}, \tag{5}$$

where R_{soil} and R_{25} are the soil respiration rate under T_s and 25 °C, respectively; T_s is soil temperature in °C; $f(\theta)$ is the respiration reduction function due to water stress; and Q_{10} is a temperature-dependent parameter, given by Kirschbaum [46] as,

$$Q_{10}(T) = \exp\left[10\beta\left(1 - \frac{T}{T_{opt}}\right)\right]. \tag{6}$$

Plant respiration (R_e) is evaluated empirically using

184
$$R_{e} = (a + bLAI)\theta_{10}e^{c(T_{s} - T_{s,ref})}, \tag{7}$$

where a = 0.159, b = 0.064, c = 0.054, and $T_{s,ref} = 27.7$ °C are empirical coefficients [53].

The total urban vegetation coverage is divided into fractions of ground vegetation (e.g. lawns) and trees, denoted as f_v and $4r_T$, respectively, as shown in Fig. 1. The urban gross primary productivity (GPP_U) and total respiration (R_{tot}) from soil and plants are determined as

$$GPP_{U} = w(4r_{T}GPP_{T} + f_{v}GPP_{G}), \qquad (8)$$

190 and

186

187

188

192

193

$$R_{\text{tot}} = w \left(f_s R_{\text{soil}} + 4 r_{\text{T}} R_{\text{T}} + f_{\nu} R_{\text{G}} \right), \tag{9}$$

respectively. The subscripts U, T, G, and 'soil' denote parameters of urban (total), tree, grass, and soil, respectively. The urban biogenic net ecosystem exchange (NEE, defined as the net CO₂

efflux) from each component, i.e. bare soil, ground level grass, and tree, is calculated separately and then aggregated using areal means to estimate total urban CO₂ flux (NEE_U) as

$$NEE_{U} = R_{tot} - GPP_{U}.$$
 (10)

We followed the sign convention commonly used in the ecological literature, i.e. both R_{tot} and GPP_U are non-negative; the negative value of NEE_U means a net carbon sink. For better clarity, both 'lower NEE' and 'higher GPP' describe the actual increase in CO_2 uptake hereafter.

Theoretically, plants under abundant radiation, ideal temperature, and less environmental (water, nutrition, etc.) stresses tend to have higher net CO₂ uptake rate, though such conditions promote the respiration rate as well. Treating urban trees separately from the ground vegetation therefore permits more accurate modeling to their corresponding growing environment and capturing different plant physiological functions more realistically. More specifically, the shading and evaporative cooling effects provided by trees alter the micrometeorological condition in street canyon, leading to less solar radiation and lower ambient temperature at the ground (road) level; both are unfavorable to ground vegetation. This intricate balance and tradeoff between cooling of urban environment and CO₂ exchange, as well as the CO₂ uptake and release, need careful investigation, and are what we aim to disentangle in subsequent simulations.

2.2 Markov chain Monte Carlo subset simulation

The conventional (and most straightforward) method to quantify the sensitivity of the proposed UCM-CO₂ model, is tuned individual parameters one at a time while keep the rest of the parameter space intact. An example is shown in Fig. 2 how the model output of NEE and its decomposed contribution from grasses, trees and soils vary with two key model parameters, viz.

the canyon aspect ratio (h/w) and the tree crown size (r_T). The advantage of this method is that the model response can be visualized intuitively with the change of the selected parameter. However, when the parameter space grows (c.f. Table 1 for a partial list of UCM-CO₂ model input parameters), the conventional sensitivity analysis is susceptible to the curse of dimensionality: the computational cost will increase exponentially with the increase of the size of the parameter space. In particular, it becomes extremely difficult for the conventional method to capture or evaluate critical responses of complex modeling framework to changes in external forcing, i.e. the occurrence of extreme events in model output with low probability of exceedance.

In the study, we resort to the stochastic subset simulation [34, 35] based on advanced MCMC algorithms to overcome the difficulties of conventional sensitivity analysis by, viz. (1) avoiding the curse of dimensionality, and (2) to capture critical model responses with low exceedance probability. Originally, the method is designed to assess the failure rate of the extreme events in engineering dynamic problems [34, 35, 47]. Its history of evolution and continuous expanding frontier of applications proved the subset simulation is versatile enough to handle problem in many different branches of engineering applications, ranging from building dynamics to environmental studies.

Here we follow a well-developed protocol of applying the subset simulation to single-layer UCMs from prior research [4, 36, 37]. The basic principle of the subset simulation and key procedure of its applications to our specific modeling framework of UCM-CO₂ are briefly described as follows. First, we need to determine the subset of stochastic UCM-CO₂ model parameters that can regulate output. Note that input parameters such as meteorological forcings are treated as deterministic and will not subject to stochastic simulations. We then statistically

characterize uncertainties of the chosen stochastic parameters using appropriate probability distribution functions (pdfs). These pdfs, given the different nature of the uncertain parameters, are determined in different ways: (1) if typical field or laboratory measurements are available, pdfs will be determined (partially) empirically, such as the thermal properties of engineered materials, (2) reasonable estimates of the parameter distribution when direct measurements are not available, e.g. distributions of the street canyon geometry or vegetation fraction, and (3) reported values (or physical ranges) of parameters that are used in numerical parameterization schemes, e.g. parameters of plant physiological functions, unsaturated soil moisture properties, etc. In all cases, subjective judgement is required in determining pdfs of model parameters and their appropriate statistics (means, standard deviations, etc.).

In particular, normal (Gaussian) distributions are used to describe variables such as thermal properties of urban landscapes, soil properties, leaf area index (LAI), and modeling parameters related to photosynthesis. Mean (most probable) values of these normal pdfs are determined based on the reported values retrieved from the literature [16, 26, 30, 48] and engineering handbooks [49], while the standard deviations are set as 25% of the mean values. Parameters of urban morphology are described by uniform distributions to represent the roughly equal probability of the presence of various urban geometry. In addition, uniform distributions are used to describe minimum leaf resistance of grass and tree ($r_{min,G}$, $r_{min,T}$), based on typical values and ranges retrieved from the literature [45, 50, 51]. The list of the stochastic parameters and the pdfs for quantifying their uncertainties are shown in Table 1.

To carry out the subset simulation, we then define a critical level (p_0) , the number of simulation (n) at each level, the number of levels (N), and the monitored target (Y). At the initial phase of simulation (level 0), direct Monte Carlo is performed where each parameter is randomly

sampled from the prescribed distributions to generate n sets of parameters. In each run, the simulation records the monitored output Y and rank Y in an ascending order. The sets of parameters that produce the most extreme np_0 responses are marked as the seed for the next level. The conditional posterior distribution is constructed based on the principle of Bayesian inference, by multiply the originally prescribed distribution and the distribution fitted from the seed. The posterior distribution from level 0 will be used as the prior distribution for generating samples for the next level of subset simulation using MCMC algorithm (from level 1 onwards). At level j, the exceedance probability is defined as $P(Y>y_j)$. The subset simulation proceeds through each conditional level until the desired exceedance probability (p_0^n) is achieved.

To quantify the sensitivity of each stochastic parameter, we adopted the index, called Percentage Sensitivity Index (PSI) defined by [36],

PSI =
$$\frac{1}{N} \sum_{j=1}^{N} \frac{E[X \mid Y > y_j] - E[X]}{E[X]}$$
, (5)

where E[X] is the prescribed mean of the parameter, y_j is the critical response at conditional level j. The PSI is calculated as the arithmetical mean of the parameter values that deviated from the prescribed value across all conditional levels.

3 Result and Discussion

To analyze the model sensitivity, the UCM-CO₂ model was driven using a sample set of meteorological forcing from the eddy covariance measurement of two consecutive clear days (2012-05-10 17:00 to 2012-05-12 17:00 local time) in Phoenix, Arizona. The weather conditions represent the typical hot and dry climate during pre-monsoon in the southwest America (Fig. 3) [52]. The subset simulation generates all 29 stochastic parameters (listed in Table 1) in each realization using the MCMC procedure, sampled individually from the prescribed pdfs. For each

realization, the model UCM-CO₂ model imports one set of 29 stochastic parameters and, together with other (deterministic) ones in the parameter space, and numerically solves the prognostic equations of heat, moisture, and carbon exchange. The model output is sampled at an interval of 30 minutes. The first 7 hours of simulations were used as the spin-up period of the model to achieve the energy balance of canyon subfacets. After the spin-up, results of a complete diurnal cycle (2012-05-11 00:00 to 2012-05-12 00:00 local time) were selected for subsequent analysis, with the effect of initial conditions adequately damped.

In all subsequent simulations, we use a conditional probability of $p_0 = 0.1$ and run 500 samples at the initial level and 450 samples in higher levels until the target exceedance probability 10^{-4} (representing the extreme events of one out of 10,000) is attained. The monitored model output, viz. the target Y, include the hourly peak and diurnal cumulative values of urban biogenic net ecosystem exchange (NEE_U), urban gross primary production (GPP_U), and total respiration (R_{tot}), respectively. For each output, we conduct and sample an ensemble of 40 runs, each containing 1400 realization of a parameter space of 29 stochastic parameters, for subsequent analysis.

3.1 The peak hourly CO₂ exchange

We first evaluate the strength of carbon fixation by the CO_2 uptake rate at the peak hour. The results of exceedance probability of monitored model output and the corresponding model sensitivity in terms of PSI values are shown in Figs. 4a and 5, respectively. The threshold values of maximum hourly NEE responding to the exceedance probability of 10^{-1} , 10^{-2} , and 10^{-3} response are -3.0 mg m⁻² s⁻¹, -5.4 mg m⁻² s⁻¹, and -7.6 mg m⁻² s⁻¹, respectively (Fig. 4a). The hourly GPP is constantly lower than the hourly NEE at each conditional level (Fig. 4a). The key

factors that enhance the CO₂ uptake are canyon width (w), tree crown size (r_T), tree height (h_T), initial soil moisture (θ_i), and tree leaf area index (LAI_T), with PSI values greater than 10% (Fig. 5). It is noteworthy that these parameters promote the CO₂ uptake via different pathways. For example, wider canyon width, larger tree crown, and denser leaves all tend to increase the biomass of tree, while taller trees lead to lower NEE since they are less shaded by canyon walls. The importance of irrigation is also underscored in the simulations, as to maintain the initial (half saturated) soil moisture θ_i . At the NEE (or GPP) peak hours, plant needs to open stomata to absorb CO₂, meanwhile lose water passively. Once feeling water stress, plant will close the stomata to conserve water, thus reduce the CO₂ uptake rate.

Thermal properties of urban landscape materials are important to regulate the thermal environment (temperature and heat fluxes) in the UCM, as reported in prior study [36]. In contrast, they are found to be relatively insignificant in this study, with PSI values less than 5%, to influence CO₂ exchange in the built environment. The impact of thermal properties are indirect: their variability leads to changes in the ambient temperature and radiative heat flux that, in turn, alter the physiological functions of plants; the latter are less sensitive to thermal conditions due to their broad adaptability. In comparison, the fraction of vegetation plays a direct role in enhancing the carbon exchange in urban areas, the increase in both LAI_T and LAI_G lead to higher NEE and GPP (Fig. 5).

One interesting finding is that the presence of urban trees, being effective in ameliorating the urban thermal environment (e.g. UHI mitigation) via shading and evaporative cooling, on the other hand offsets the enhancement of CO_2 uptake by a warmer environment. Among all species-dependent parameters in photosynthesis modeling (Table 1), the hourly peak CO_2 assimilation rate is most sensitive to $r_{min,T}$, indicating the minimum leaf resistance is a key parameter in CO_2

uptake modeling, especially at fine temporal resolution. The model sensitivity to $r_{\min,T}$ is diminished when considering the daily CO₂ exchange (to be discussed in Section 3.2).

In the UCM-CO₂ modeling framework, as well as in many real urban settings, urban trees usually have a higher biomass density and more rapid CO₂ uptake rate than their counterpart of ground vegetation. In addition, urban trees (especially crowns) benefit from their higher location in street canyons, thus receiving more solar energy than ground level vegetation. This urban physics is manifest in the results of our simulations in Fig. 5, where we found the model sensitivity of peak hour output is dominated by tree parameters: Parameters denoting ground vegetation (grass), viz. f_v , LAI_G, and $r_{min,G}$, are not as sensitive as those parameters of trees (r_T , LAI_T, $r_{min,T}$).

To maximize net CO₂ uptake, total respiration (sum of the respiration from grass, tree, and soil) needs to be suppressed while promoting the CO₂ assimilation rate. However, in most cases, the rate of photosynthesis and respiration are positively related as they partially shared the series of biochemical reactions inside of the plants. In the numerical simulation, higher initial soil moisture (more irrigation) will promote GPP and R_{tot} in the same time since it provides a favored growing condition for plant as well as the microbes in soil. Nevertheless, our numerical simulations identified some parameters that have opposite effect on the plant and soil carbon dynamics, the soil fraction (f_s) being the critical one. The soil fraction played a vital role in CO₂ budget as microbes in bare soil could be the largest carbon source in urban street canyon [27]. A larger fraction of bare soil in urban areas competes for available space for vegetation, hence reduce the CO₂ sink strength of plants while releasing more CO₂ into the atmosphere. The other parameter that has the opposite effect is the tree height h_T : taller trees enhance the plant carbon uptake but suppress total respiration.

3.2 The diurnal cumulative CO₂ exchange

In a diurnal cycle, the CO₂ exchange is most active from noon to early afternoon with the optimal growing conditions during this time window (if without water stress). However, in hot environment, the excessive high temperature will force plant to close the stomata, thus lower the photosynthesis rate. The situation is not manifest when only examining the peak hour model output in Section 3.1. In this section, we further exam the model output of the diurnal cumulative (daily) CO₂ budgets and probe into the sensitivity to parameter uncertainties.

Figure 4b shows the critical response of daily NEE, GPP and R_{tot} with the corresponding exceedance probability. Daily NEE can be positive (net CO_2 source) when the respiration is high. A sharp decrease of NEE is observed when the exceedance probability is greater than 0.7, making the daily NEE negative (net CO_2 sink) for most of urban scenarios. Daily CO_2 exchanges (NEE_U, GPP_U and R_{tot}) exhibit steady changes with the increase of exceedance probability, which are similar to the peak hourly CO_2 exchanges at smaller exceedance probabilities.

The results of sensitivity analysis in terms of PSI for daily cumulative carbon exchange are shown in Fig. 6. In general, the model sensitivity to most parameters remains roughly for the diurnal average output as compared to hourly peaks, indicating the over robustness of the UCM- CO_2 modeling framework and common characteristics of model physics at different time scales. For example, the diurnal urban carbon dynamics remain relatively insensitive to all thermal properties. In addition, the soil fraction f_s plays similar role in regulating the plant carbon exchange (negative correlation) and total respiration (positive) at the daily scale.

Nevertheless, there are some noticeable differences in the model sensitivity to some parameters at the diurnal scale (Fig. 6) in comparison to the peak hourly output (Fig. 5). Firstly,

the average absolute values of PSI for the daily NEE across the entire parameter space is smaller than that for the peak hourly NEE (8.0% vs 5.2%), indicating a decrease in overall model sensitivity when aggregated over longer time span. Secondly, the relative sensitivity among the parameter space has altered. The vegetation fraction (f_v) out-weighted tree parameters (r_T and h_T), LAI values, initial soil moisture, and canyon building height (h), becoming the second most sensitive parameter in the test. The increase of f_v reduces the coverage of bare soil or paved surfaces, providing greater biomass for CO₂ assimilation while shrinking the soil respiration. Besides, the modeling parameter, $r_{\min,T}$, is not sensitive to the daily NEE, though showing a high PSI value in terms of the peak hourly NEE. Comparing to the other physical parameters in the UCM-CO₂ model, the model parameters of plant, such as $r_{\min,T}$, admit less clear physical interpretation. In general, it is preferred that the uncertainty of these parameters of plant physiological functions, mostly empirically based, should be mitigated to improve the robustness of predicting urban carbon dynamics.

In Fig. 6, the PSI value of tree crown radius ($r_{\rm T}$) becomes negative in terms of daily NEE, though the magnitude is small (-2.2%), (the value is significantly positive in peak hourly NEE output, c.f. Fig. 5) This change reflects that an excessive increase in urban tree biomass tends to deteriorate the growing condition and physiological functions of the ground vegetation, primarily due to the tree shading effect. It is noteworthy that $r_{\rm T}$ is also negatively correlated to the daily total respiration rate, with a PSI of -16.5%. As soil and plant respirations are strongly (positively) correlated to the ambient temperature near the canyon ground, the cooling effect induced by tree shading at the ground level also reduces the respiration rate, thus decrease the average NEE over the diurnal cycle.

3.3 Implications of the sensitivity analysis

The main findings from the results of sensitivity analysis, as discussed above, are quantitatively consistent to those reported, albeit scattered, in the literature. In addition, the uncertainty characterization and results of sensitivity analysis can provide important guideline to future development of the coupled UCM-CO₂ model. One important application is to use PSI to inform model calibration by focusing on the critical subset of parameters (e.g. those of urban vegetation) for capturing more realistic urban carbon dynamics. Though focusing on the CO₂ exchange, results of subset simulations also reveal complex interplay among urban morphology, vegetation dynamics, thermal environment, and possible planning strategies, and have important implications to sustainable urban development and the co-benefits of mitigating heat and carbon emissions. These implications include: (1) certain urban morphology, in particular lower building heights and/or wider streets, can help to strengthen plant physiological functions as carbon sinks but also increase total respiration rate; (2) replacing bare soil fraction in urban areas by green vegetation, using either lawns or trees, appears to be very desirable for urban planning as to mitigate both heat and carbon emissions; and (3) one particular urban greening strategy, viz. the plantation of tall urban trees with larger crown sizes, emerges as the most effective means in reducing peak carbon emission and suppressing soil respiration. Trees with too large crown sizes, however, can sometimes lead to unintended consequence of suppressing photosynthesis of grass at the ground level and reduce the overall carbon uptake capacity by urban vegetation.

421

422

401

402

403

404

405

406

407

408

409

410

411

412

413

414

415

416

417

418

419

420

4 Concluding remarks

In this study, we characterized the uncertainty of the parameter space and conducted a sensitivity analysis of a newly developed UCM-CO₂ model (Li and Wang, 2020) using the subset simulation. In particular, we focused on the dynamics of plant CO₂ exchange by monitoring the model output of peak hourly and daily cumulative carbon fluxes in terms of net ecosystem exchange, gross primary productivity, and total respiration. It is noteworthy that the UCM-CO₂ model is capable of resolving the anthropogenic heat and CO₂ fluxes arising from traffic emissions and building operations based on gridded dataset. The anthropogenic heat and carbon emissions can affect the growing conditions of urban vegetation by altering the concentration of trace gases, thermal environment, particle deposition, and flow field in the urban canopy layer. On the other hand, the modified plant physiological functions and the concomitant changes in the urban thermal environment and carbon concentration can, in turn, regulate anthropogenic heat and carbon emissions. Disentangling this two-way interaction between anthropogenic and biogenic sources of heat and carbon emissions remains an outstanding challenge and calls for further development of more sophisticated urban modeling frameworks.

423

424

425

426

427

428

429

430

431

432

433

434

435

436

437

438

439

440

441

442

443

444

445

From the results of the sensitivity study, urban morphology, urban vegetation fraction and geometry (especially those of trees), and soil fraction, are of pivotal importance in determining the prediction of urban carbon dynamics. In contrast, thermal parameters of urban landscapes, albeit being critical in regulating the thermal environment of urban areas, have indirect and relatively insignificant influence on carbon dynamics. As biophysical functions of urban vegetation play a critical role in modulating both heat and carbon emissions, they also exhibit complex interactions with the built environment in the urban surface layer. While the current study shade some lights on this aspect, it remains an outstanding challenge for future UCM-CO₂

modeling development to further disentangle the interactions of anthropogenic and biogenic processes, as well as to promote sustainable urban development strategies that maximize the cobenefits of mitigating heat and carbon emissions and improve the overall environmental quality.

Acknowledgement

This study is based upon work supported by the National Science Foundation under Grant #

AGS-1930629 and CBET-2028868. The authors also acknowledge the Central Arizona-Phoenix

Long-Term Ecological Research (CAP-LTER) project for providing the observational dataset used in this study. The dataset can be accessed from the data portal at https://sustainability.asu.edu/caplter/research/long-term-monitoring/urban-flux-tower/.

Table 1. Statistics of selected uncertain parameters. The unit of leaf resistance is in mm s⁻¹. The unit of thermal conductivity and heat capacity are W m⁻¹ K⁻¹ and MJ m⁻³ K⁻¹, respectively. The other parameters are dimensionless.

Parameter		PDF	Mean	Std.	Min.	Max.
Canyon g	geometry					
w	Normalized road width	Uniform	0.425		0.05	0.8
h	Normalized building height	Uniform	0.8		0.1	1.5
Soil prop	erties					
$f_{ m s}$	Bare soil fraction	Uniform	0.275		0.05	0.5
θ_s	Saturation soil moisture	Normal	0.35	0.0875	0.15	0.55
$ heta_r$	Residual soil moisture	Normal	0.06	0.015	0.02	0.1
Plant pro	perties					
$f_{ m v}$	Vegetated fraction	Uniform	0.275		0.05	0.5
r_{T}	Normalized tree crown radius	Uniform	0.07		0.02	0.12
$h_{ m T}$	Normalized tree height	Uniform	0.625		0.25	1
x_{T}	Normalized tree location	Uniform	0.5		0	1
LAI_{G}	Grass - leaf area index	Normal	2.5	1	1.00	5.00
LAI_T	Tree - leaf area index	Normal	4	1	1.50	6.50
$ heta_i$	Initial soil moisture	Uniform	0.19		0.08	0.3
Photosyn	thesis modeling					
CF	PAR conversion factor	Normal	0.5	0.125	0.3	0.7
Kx_T	Tree - LAI extinction coefficient	Normal	0.48	0.12	0.28	0.68
$r_{\min,T}$	Tree - minimum leaf resistance	Uniform	175		150	200
Kx_G	Grass - LAI extinction coefficient	Normal	0.48	0.12	0.28	0.68
$r_{\rm min,G}$	Grass - minimum leaf resistance	Uniform	205		180	230
Subfacet	thermal properties					
aW	Albedo - wall	Normal	0.17	0.04	0.06	0.28
aG_1	Albedo - paved	Normal	0.125	0.03	0.05	0.20
aG_2	Albedo - bare soil	Normal	0.2	0.05	0.08	0.33
aG_3	Albedo - vegetated	Normal	0.2	0.05	0.08	0.33
kW	Thermal conductivity - wall	Normal	0.12	0.03	0.05	0.20
kG_1	Thermal conductivity - paved	Normal	1.5	0.38	0.56	2.44
kG_2	Thermal conductivity - bare soil	Normal	0.65	0.16	0.24	1.06
kG_3	Thermal conductivity - vegetated	Normal	0.22	0.06	0.08	0.36
cW	Heat capacity - wall	Normal	2.3	0.58	0.86	3.74
cG_1	Heat capacity - paved	Normal	0.9	0.23	0.34	1.46
cG_2	Heat capacity - bare soil	Normal	1.7	0.43	0.64	2.76
cG_3	Heat capacity - vegetated	Normal	1	0.25	0.38	1.63

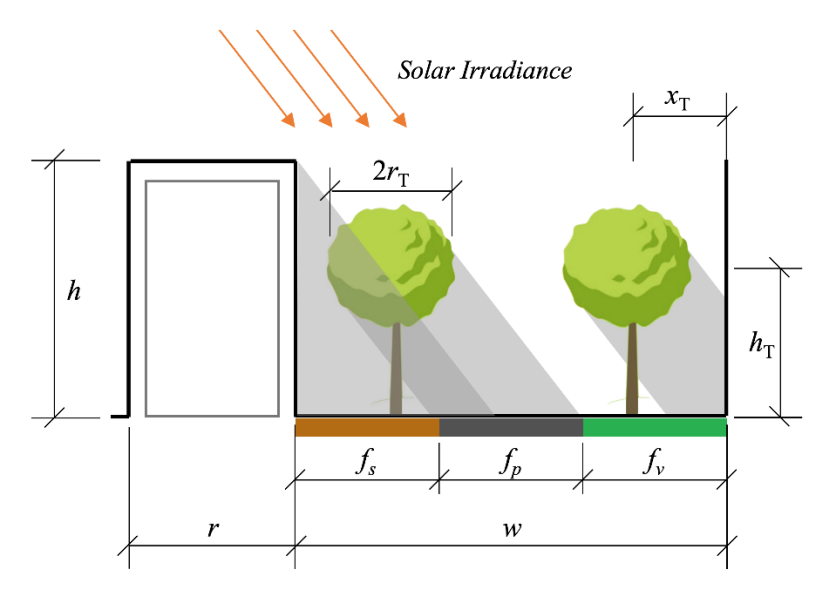


Figure 1. Representative urban street canyon used in the coupled UCM-CO₂ model. h, r, w, h_T, r_T, and x_T are the normalized building height, building roof width, street width, tree height, tree crown radius, and tree location, respectively. f_S, f_P, and f_V are the normalized bare soil fraction, pavement fraction, and vegetation fraction of the canyon ground, respectively.

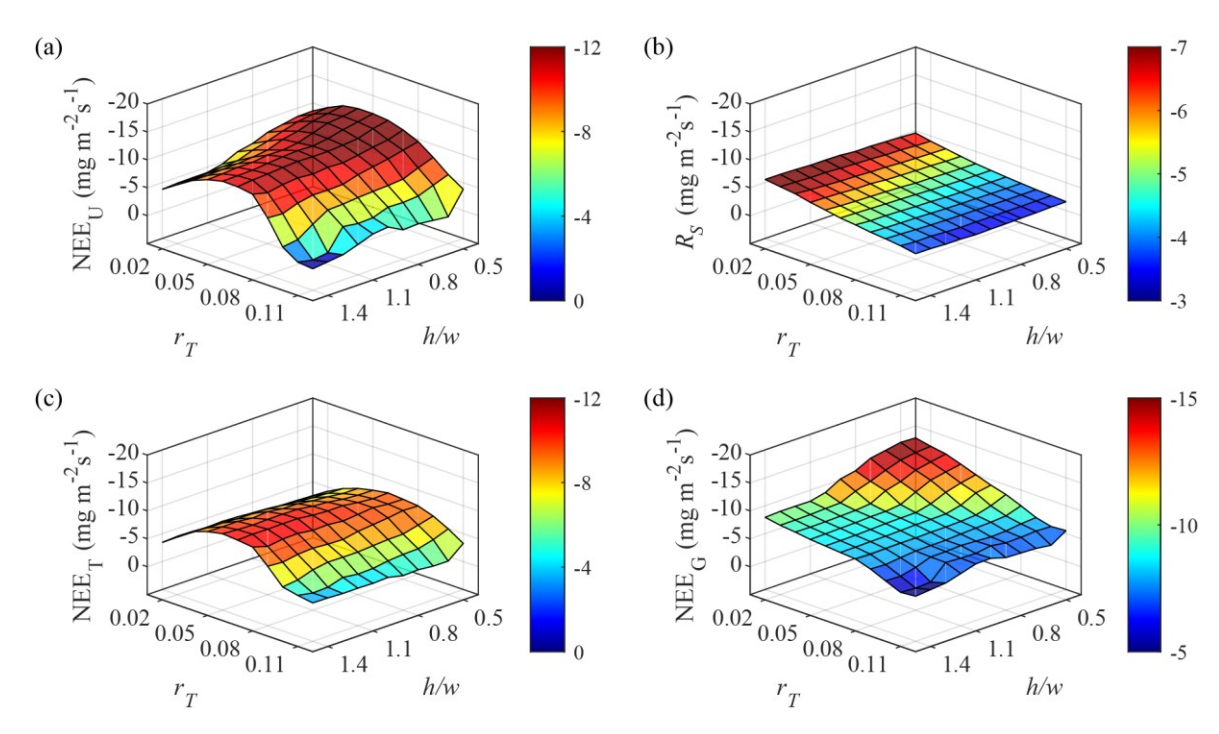


Figure 2. The variation of (a) NEE over urban area (NEE_U), (b) Soil respiration per urban area $(R_S = wf_sR_{soil})$, (c) NEE from tall trees (NEE_T), and (d) NEE from ground vegetation (NEE_G) in terms of the change in normalized tree crown radius (r_T) and canyon aspect ratio (h/w).

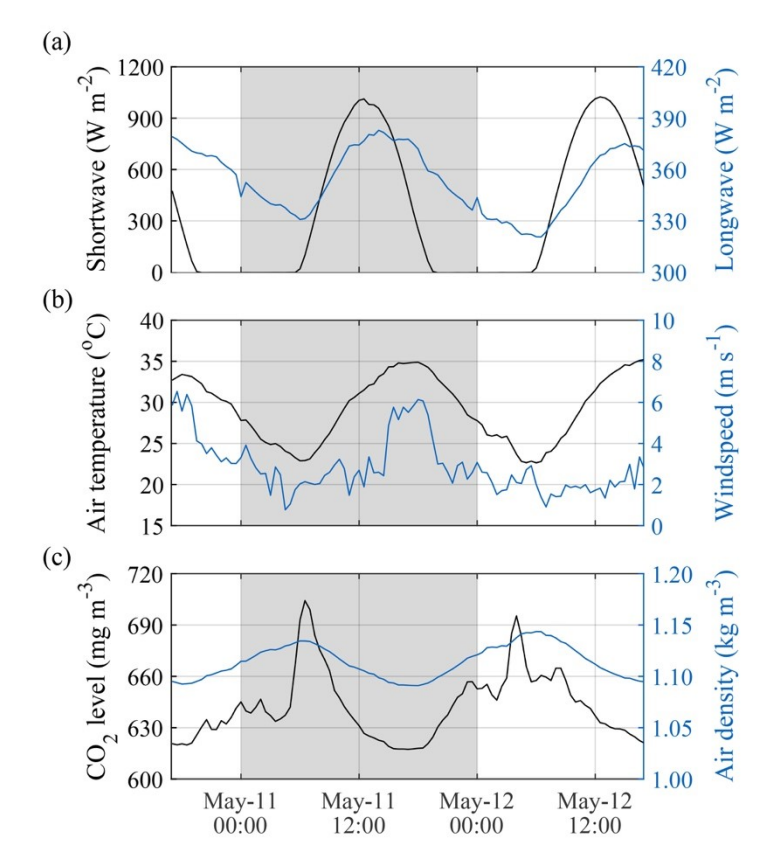


Figure 3. Atmospheric forcing used in subset simulation measured at west of downtown Phoenix in 2012 (33.483847°N,112.142609°W). (a) Downwelling radiations; (b) Air temperature and windspeed; (c) CO₂ concentration and air density. Time showed in the figure is local time (UTC -7). Only the results during the shaded period are discussed in the study, while the non-shaded period is used for quality control. A detail description of the measurement site can be found in Chow et al. (2014).

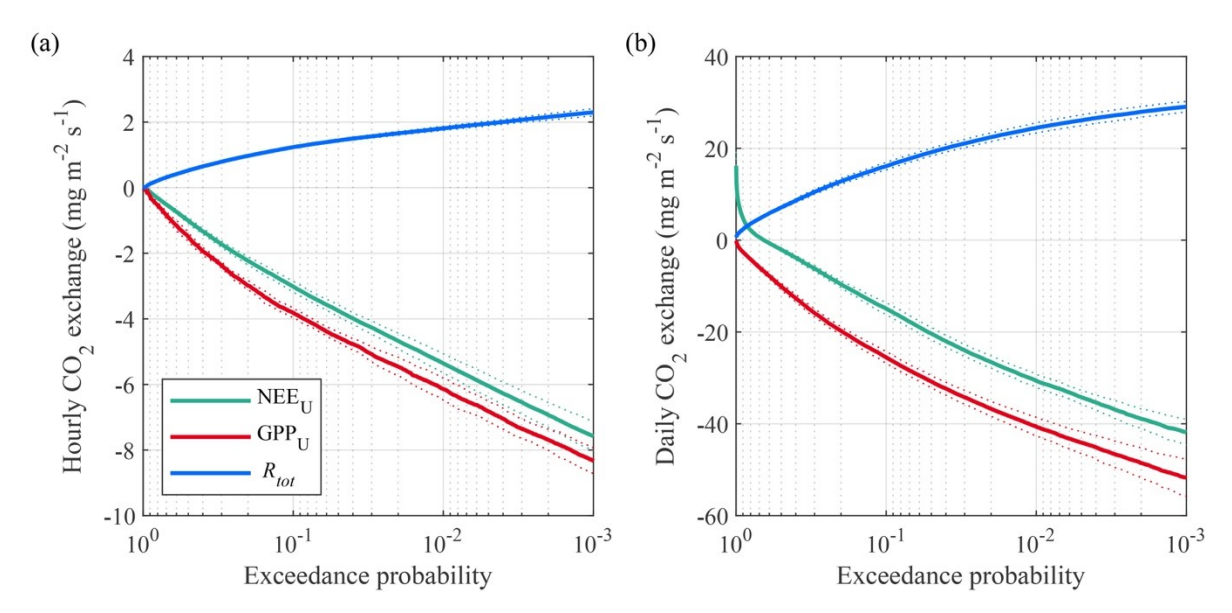


Figure 4. The exceedance probability of (a) the hourly maximum, and (b) the daily cumulative values of NEE_U, GPP_U, and R_{tot} respectively. The dashed line shows one standard deviation (\pm 1 σ) from the ensemble means.

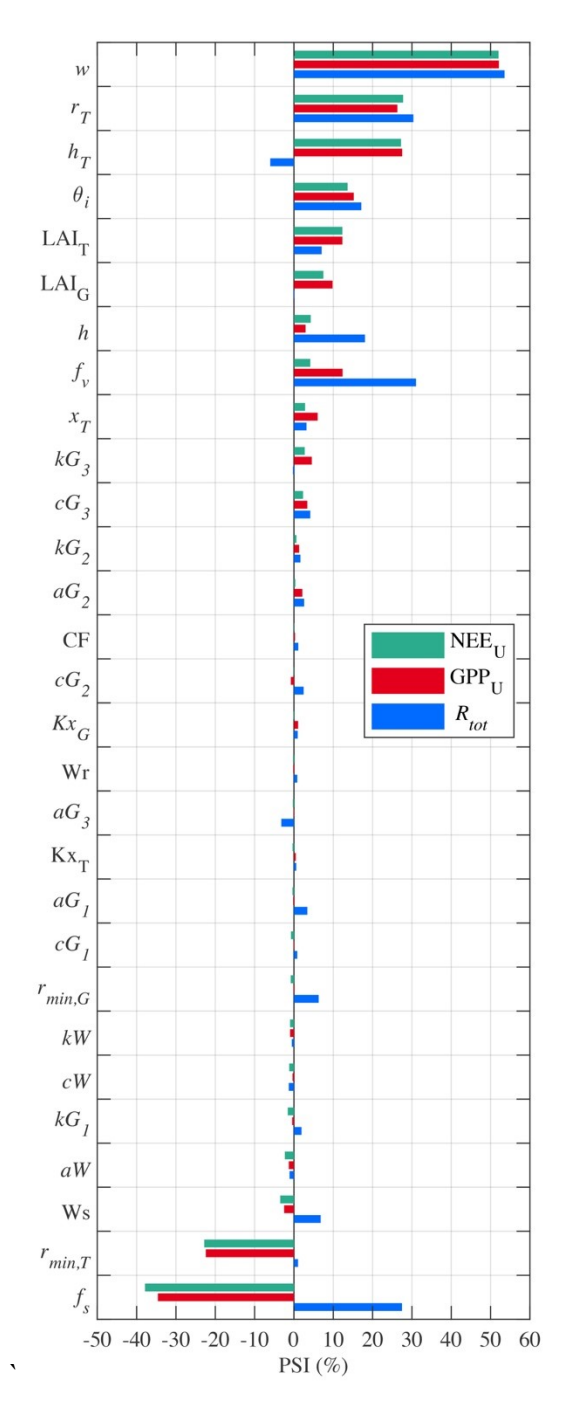


Figure 5. PSI values when the simulation targets are NEE_U, GPP_U and R_{tot} at the peak hour in a day. The order is ranked based on the PSI values of NEE_U at the peak hour.

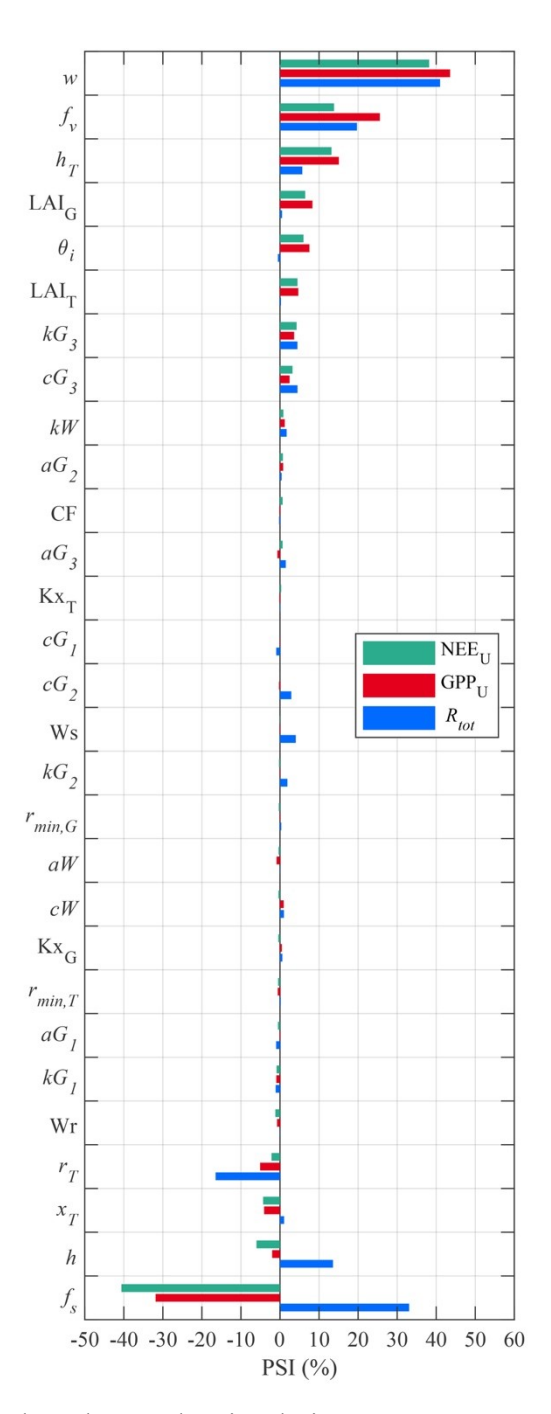


Figure 6. Same as Figure 5 but change the simulation targets to NEE_U, GPP_U and R_{tot} of the daily total. The order is ranked based on the PSI values of NEE_U of the daily total.

References

- 487 [1] United Nations Human Settlements Programme (UN-Habitat), Global report on human
- settlements 2011: cities and climate change. (2011) London, United Kingdom.
- 489 [2] G. Churkina, Modeling the carbon cycle of urban systems, Ecol. Modell. 216 (2008) 107-
- 490 113, http://doi.org/10.1016/j.ecolmodel.2008.03.006
- 491 [3] J. Song, Z.-H. Wang, Impacts of mesic and xeric urban vegetation on outdoor thermal
- comfort and microclimate in Phoenix, AZ, Build. Environ. 94 (2015) 558-568,
- 493 http://doi.org/10.1016/j.buildenv.2015.10.016
- 494 [4] J. Song, Z.H. Wang, Evaluating the impact of built environment characteristics on urban
- boundary layer dynamics using an advanced stochastic approach, Atmos. Chem. Phys. 16
- 496 (2016) 6285-6301, http://doi.org/10.5194/acp-16-6285-2016
- 497 [5] E.C. Lahr, R.R. Dunn, S.D. Frank, Variation in photosynthesis and stomatal conductance
- among red maple (Acer rubrum) urban planted cultivars and wildtype trees in the
- southeastern United States, PLOS ONE 13 (2018) e0197866,
- 500 http://doi.org/10.1371/journal.pone.0197866
- 501 [6] L. Meng, J. Mao, Y. Zhou, A.D. Richardson, X. Lee, P.E. Thornton, . . . G. Jia, Urban
- warming advances spring phenology but reduces the response of phenology to
- temperature in the conterminous United States, Proc. Natl. Acad. Sci. U. S. A. 117 (2020)
- 504 4228, http://doi.org/10.1073/pnas.1911117117
- 505 [7] S. Zhao, S. Liu, D. Zhou, Prevalent vegetation growth enhancement in urban
- environment, Proc. Natl. Acad. Sci. U. S. A. 113 (2016) 6313,
- 507 http://doi.org/10.1073/pnas.1602312113

[8] A.M. Luketich, S.A. Papuga, M.A. Crimmins, Ecohydrology of urban trees under passive 508 and active irrigation in a semiarid city, PLOS ONE 14 (2019) e0224804, 509 http://doi.org/10.1371/journal.pone.0224804 510 [9] H. Wang, I.C. Prentice, T.F. Keenan, T.W. Davis, I.J. Wright, W.K. Cornwell, . . . C. 511 Peng, Towards a universal model for carbon dioxide uptake by plants, Nat. Plants 3 512 513 (2017) 734-741, http://doi.org/10.1038/s41477-017-0006-8 S. Wang, W. Ju, J. Peñuelas, A. Cescatti, Y. Zhou, Y. Fu, ... Y. Zhang, Urban-rural [10] 514 gradients reveal joint control of elevated CO₂ and temperature on extended 515 photosynthetic seasons, Nat. Ecol. Evol. 3 (2019) 1076-1085, 516 http://doi.org/10.1038/s41559-019-0931-1 517 C.S.B. Grimmond, M. Best, J. Barlow, A.J. Arnfield, J.-J. Baik, A. Baklanov, . . . T. 518 [11] Williamson, Urban surface energy balance models: model characteristics and 519 methodology for a comparison study, in Meteorological and Air Quality Models for 520 Urban Areas, A. Baklanov, et al., Editors. 2009, Springer Berlin Heidelberg: Berlin, 521 Heidelberg. p. 97-123. 522 523 [12] E. Redon, A. Lemonsu, V. Masson, An urban trees parameterization for modeling 524 microclimatic variables and thermal comfort conditions at street level with the Town Energy Balance model (TEB-SURFEX v8.0), Geosci. Model Dev. 13 (2020) 385-399, 525 http://doi.org/10.5194/gmd-13-385-2020 526 527 [13] C. Wang, Z.-H. Wang, J. Yang, Cooling effect of urban trees on the built environment of

contiguous United States, Earth's Future 6 (2018) 1066-1081,

http://doi.org/10.1029/2018EF000891

528

529

C. Wang, Q. Li, Z.-H. Wang, Quantifying the impact of urban trees on passive pollutant 530 [14] dispersion using a coupled large-eddy simulation—Lagrangian stochastic model, Build. 531 Environ. 145 (2018) 33-49, http://doi.org/10.1016/j.buildenv.2018.09.014 532 S.-H. Lee, S.-U. Park, A vegetated urban canopy model for meteorological and [15] 533 environmental modelling, Boundary Layer Meteorol. 126 (2008) 73-102, 534 535 http://doi.org/10.1007/s10546-007-9221-6 A. Lemonsu, V. Masson, L. Shashua-Bar, E. Erell, D. Pearlmutter, Inclusion of [16] 536 vegetation in the Town Energy Balance model for modelling urban green areas, Geosci. 537 Model Dev. 5 (2012) 1377-1393, http://doi.org/10.5194/gmd-5-1377-2012 538 R. Upreti, Z.-H. Wang, J. Yang, Radiative shading effect of urban trees on cooling the [17] 539 regional built environment, Urban For. Urban Green 26 (2017) 18-24, 540 http://doi.org/10.1016/j.ufug.2017.05.008 541 C.S.B. Grimmond, T.S. King, F.D. Cropley, D.J. Nowak, C. Souch, Local-scale fluxes of [18] 542 543 carbon dioxide in urban environments: methodological challenges and results from Chicago, Environ. Pollut. 116 (2002) S243-S254, http://doi.org/10.1016/S0269-544 7491(01)00256-1 545 546 [19] D.E. Pataki, D.R. Bowling, J.R. Ehleringer, Seasonal cycle of carbon dioxide and its isotopic composition in an urban atmosphere: anthropogenic and biogenic effects, J. 547 548 Geophys. Res. Atmos. 108 (2003) http://doi.org/10.1029/2003JD003865 549 [20] D.E. Pataki, D.R. Bowling, J.R. Ehleringer, J.M. Zobitz, High resolution atmospheric 550 monitoring of urban carbon dioxide sources, Geophys. Res. Lett. 33 (2006) http://doi.org/10.1029/2005GL024822 551

[21] M. Jung, C. Schwalm, M. Migliavacca, S. Walther, G. Camps-Valls, S. Koirala, . . . M. 552 Reichstein, Scaling carbon fluxes from eddy covariance sites to globe: synthesis and 553 evaluation of the FLUXCOM approach, Biogeosciences 17 (2020) 1343-1365, 554 http://doi.org/10.5194/bg-17-1343-2020 555 [22] C. Gately, L.R. Hutyra, I.S. Wing, DARTE annual on-road CO₂ emissions on a 1-km 556 557 grid, conterminous USA V2, 1980-2017. 2019, ORNL Distributed Active Archive Center, http://doi.org/10.3334/ORNLDAAC/1735 558 K.R. Gurney, D.L. Mendoza, Y. Zhou, M.L. Fischer, C.C. Miller, S. Geethakumar, S. de [23] 559 la Rue du Can, High resolution fossil fuel combustion CO₂ emission fluxes for the United 560 States, Environ. Sci. Technol. 43 (2009) 5535-5541, http://doi.org/10.1021/es900806c 561 [24] T. Oda, S. Maksyutov, R.J. Andres, The Open-source Data Inventory for Anthropogenic 562 CO₂, version 2016 (ODIAC2016): a global monthly fossil fuel CO₂ gridded emissions 563 data product for tracer transport simulations and surface flux inversions, Earth Syst. Sci. 564 565 Data 10 (2018) 87-107, http://doi.org/10.5194/essd-10-87-2018 L.E. Mitchell, J.C. Lin, D.R. Bowling, D.E. Pataki, C. Strong, A.J. Schauer, ... J.R. [25] 566 Ehleringer, Long-term urban carbon dioxide observations reveal spatial and temporal 567 568 dynamics related to urban characteristics and growth, Proc. Natl. Acad. Sci. U. S. A. 115 (2018) 2912, http://doi.org/10.1073/pnas.1702393115 569 570 [26] M. Goret, V. Masson, R. Schoetter, M.-P. Moine, Inclusion of CO₂ flux modelling in an 571 urban canopy layer model and an evaluation over an old European city centre, Atmos. Environ. X 3 (2019) 100042, http://doi.org/10.1016/j.aeaoa.2019.100042 572

- 573 [27] P. Li, Z.-H. Wang, Modeling carbon dioxide exchange in a single-layer urban canopy
- 574 model, Build. Environ. 184 (2020) 107243,
- 575 http://doi.org/10.1016/j.buildenv.2020.107243
- 576 [28] H. Kusaka, H. Kondo, Y. Kikegawa, F. Kimura, A simple single-layer urban canopy
- model for atmospheric models: comparison with multi-layer and slab models, Boundary
- 578 Layer Meteorol. 101 (2001) 329-358, http://doi.org/10.1023/A:1019207923078
- 579 [29] V. Masson, A physically-based scheme for the urban energy budget in atmospheric
- 580 models, Boundary Layer Meteorol. 94 (2000) 357-397,
- 581 http://doi.org/10.1023/A:1002463829265
- 582 [30] Z.-H. Wang, E. Bou-Zeid, J.A. Smith, A coupled energy transport and hydrological
- model for urban canopies evaluated using a wireless sensor network, Q. J. R. Meteorol.
- Soc. 139 (2013) 1643-1657, http://doi.org/https://doi.org/10.1002/qj.2032
- 585 [31] J. Yang, Z.-H. Wang, F. Chen, S. Miao, M. Tewari, J.A. Voogt, S. Myint, Enhancing
- 586 hydrologic modelling in the coupled Weather Research and Forecasting–urban modelling
- system, Boundary Layer Meteorol. 155 (2015) 87-109, http://doi.org/10.1007/s10546-
- 588 014-9991-6
- 589 [32] M.A. Bessa, R. Bostanabad, Z. Liu, A. Hu, D.W. Apley, C. Brinson, . . . Wing K. Liu, A
- framework for data-driven analysis of materials under uncertainty: countering the curse
- of dimensionality, Comput. Methods in Appl. Mech. Eng. 320 (2017) 633-667,
- 592 http://doi.org/10.1016/j.cma.2017.03.037
- 593 [33] A. Pakes, P. McGuire, Stochastic algorithms, symmetric Markov perfect equilibrium, and
- the 'curse' of dimensionality, Econometrica 69 (2001) 1261-1281,
- 595 http://doi.org/10.1111/1468-0262.00241

S.-K. Au, J.L. Beck, Estimation of small failure probabilities in high dimensions by 596 [34] subset simulation, Probabilistic Eng. Mech. 16 (2001) 263-277, 597 http://doi.org/10.1016/S0266-8920(01)00019-4 598 S.-K. Au, J.L. Beck, Subset simulation and its application to seismic risk based on [35] 599 dynamic analysis, J. Eng. Mech. 129 (2003) 901-917, 600 601 http://doi.org/10.1061/(ASCE)0733-9399(2003)129:8(901) Z.-H. Wang, E. Bou-Zeid, S.K. Au, J.A. Smith, Analyzing the sensitivity of WRF's [36] 602 single-layer urban canopy model to parameter uncertainty using advanced Monte Carlo 603 simulation, J. Appl. Meteorol. Climatol. 50 (2011) 1795-1814, 604 http://doi.org/10.1175/2011jamc2685.1 605 J. Yang, Z.-H. Wang, Physical parameterization and sensitivity of urban hydrological 606 [37] models: application to green roof systems, Build. Environ. 75 (2014) 250-263, 607 http://doi.org/10.1016/j.buildenv.2014.02.006 608 609 [38] N. Meili, G. Manoli, P. Burlando, E. Bou-Zeid, W.T.L. Chow, A.M. Coutts, . . . S. Fatichi, An urban ecohydrological model to quantify the effect of vegetation on urban 610 climate and hydrology (UT&C v1.0), Geosci. Model Dev. 13 (2020) 335-362, 611 612 http://doi.org/10.5194/gmd-13-335-2020 T. Loridan, C.S.B. Grimmond, S. Grossman-Clarke, F. Chen, M. Tewari, K. 613 [39] 614 Manning, . . . M. Best, Trade-offs and responsiveness of the single-layer urban canopy 615 parametrization in WRF: An offline evaluation using the MOSCEM optimization algorithm and field observations, Q. J. R. Meteorol. Soc. 136 (2010) 997-1019, 616

http://doi.org/10.1002/qj.614

- 618 [40] C.S.B. Grimmond, M. Blackett, M.J. Best, J.-J. Baik, S.E. Belcher, J. Beringer, . . . N.
- Zhang, Initial results from Phase 2 of the international urban energy balance model
- 620 comparison, Int. J. Clim. 31 (2011) 244-272, http://doi.org/10.1002/joc.2227
- 621 [41] C.S.B. Grimmond, M. Blackett, M.J. Best, J. Barlow, J.-J. Baik, S.E. Belcher, ... N.
- Zhang, The international urban energy balance models comparison project: first results
- from Phase 1, J. Appl. Meteorol. Climatol. 49 (2010) 1268-1292,
- http://doi.org/10.1175/2010jamc2354.1
- 625 [42] B.N. Bailey, M. Overby, P. Willemsen, E.R. Pardyjak, W.F. Mahaffee, R. Stoll, A
- scalable plant-resolving radiative transfer model based on optimized GPU ray tracing,
- 627 Agric. For. Meteorol. 198-199 (2014) 192-208,
- http://doi.org/10.1016/j.agrformet.2014.08.012
- 629 [43] Z.-H. Wang, Monte Carlo simulations of radiative heat exchange in a street canyon with
- trees, Solar Energy 110 (2014) 704-713, http://doi.org/10.1016/j.solener.2014.10.012
- 631 [44] Q. Li, Z.-H. Wang, Large-eddy simulation of the impact of urban trees on momentum
- and heat fluxes, Agric. For. Meteorol. 255 (2018) 44-56,
- http://doi.org/10.1016/j.agrformet.2017.07.011
- R.J. Ronda, H.A.R. de Bruin, A.A.M. Holtslag, Representation of the canopy
- conductance in modeling the suface energy budget for low vegetation, J. Appl. Meteorol.
- Climatol. 40 (2001) 1431-1444, http://doi.org/10.1175/1520-
- 637 0450(2001)040<1431:Rotcci>2.0.Co;2
- 638 [46] M.U.F. Kirschbaum, The temperature dependence of soil organic matter decomposition,
- and the effect of global warming on soil organic C storage, Soil Biol. Biochem. 27 (1995)
- 640 753-760, http://doi.org/10.1016/0038-0717(94)00242-S

S.-K. Au, Z.-H. Wang, S.-M. Lo, Compartment fire risk analysis by advanced Monte 641 [47] Carlo simulation, Eng. Struct. 29 (2007) 2381-2390, 642 http://doi.org/10.1016/j.engstruct.2006.11.024 643 J. Yang, Z.-H. Wang, K.E. Kaloush, H. Dylla, Effect of pavement thermal properties on [48] 644 mitigating urban heat islands: a multi-scale modeling case study in Phoenix, Build. 645 646 Environ. 108 (2016) 110-121, http://doi.org/10.1016/j.buildenv.2016.08.021 [49] 2009 ASHRAE Handbook: Fundamentals. 2009, American Society of Heating, 647 Refrigerating and Air-Conditioning Engineers, Inc. (ASHRAE). 648 [50] R.A. Duursma, C.J. Blackman, R. Lopéz, N.K. Martin-StPaul, H. Cochard, B.E. Medlyn, 649 On the minimum leaf conductance: its role in models of plant water use, and ecological 650 and environmental controls, New Phytol. 221 (2019) 693-705, 651 http://doi.org/10.1111/nph.15395 652 D.S. Niyogi, S. Raman, A. Prabhu, U. Kumar, S.S. Joshi, Direct estimation of stomatal [51] 653 resistance for meteorological applications, Geophys. Res. Lett. 24 (1997) 1771-1774, 654 http://doi.org/10.1029/97GL01790 655 W.T.L. Chow, T.J. Volo, E.R. Vivoni, G.D. Jenerette, B.L. Ruddell, Seasonal dynamics 656 [52] 657 of a suburban energy balance in Phoenix, Arizona, Int. J. Clim. 34 (2014) 3863-3880, http://doi.org/10.1002/joc.3947 658 J.M. Norman, R. Garcia, S.B. Verma, Soil surface CO₂ fluxes and the carbon budget of a 659 [53] grassland. J. Geophys. Res-Atmos. 97 (1992) 18845–18853, 660 https://doi.org/10.1029/92JD01348 661